Journal of Plant Interactions

ISSN: (Print) (Online) Journal homepage: https://www.tandfonline.com/loi/tjpi20

Overexpression of cytoplasmic *Solanum tuberosum* Glyceraldehyde 3-phosphate dehydrogenase (GAPDH) gene improves PSII efficiency and alleviates salinity stress in *Arabidopsis*.

Sajeesh Kappachery, Shina Sasi, Onoud Alyammahi, Ayesha Alyassi, Jelli Venkatesh & Mayank Anand Gururani

To cite this article: Sajeesh Kappachery, Shina Sasi, Onoud Alyammahi, Ayesha Alyassi, Jelli Venkatesh & Mayank Anand Gururani (2021) Overexpression of cytoplasmic *Solanum tuberosum* Glyceraldehyde 3-phosphate dehydrogenase (GAPDH) gene improves PSII efficiency and alleviates salinity stress in *Arabidopsis*., Journal of Plant Interactions, 16:1, 398-410, DOI: 10.1080/17429145.2021.1962420

To link to this article: https://doi.org/10.1080/17429145.2021.1962420

© 2021 The Author(s). Published by Informa UK Limited, trading as Taylor & Francis Group

View supplementary material

Published online: 17 Aug 2021.

Submit your article to this journal

Article views: 191

View related articles

View Crossmark data

Full Terms & Conditions of access and use can be found at
https://www.tandfonline.com/action/journalInformation?journalCode=tjpi20

JOURNAL OF PLANT INTERACTIONS
2021, VOL. 16, NO. 1, 398–410
https://doi.org/10.1080/17429145.2021.1962420

Taylor & Francis
Taylor & Francis Group

Plant-Soil Interactions (including Plant-Water Interactions)

OPEN ACCESS Check for updates

Overexpression of cytoplasmic *Solanum tuberosum* Glyceraldehyde 3-phosphate dehydrogenase (GAPDH) gene improves PSII efficiency and alleviates salinity stress in *Arabidopsis*.

Sajeesh Kappachery[a]*, Shina Sasi[b]*, Onoud Alyammahi[a], Ayesha Alyassi[a], Jelli Venkatesh[c] and Mayank Anand Gururani [a]

[a]Department of Biology, College of Science, UAE University, Al Ain, United Arab Emirates; [b]Khalifa Center for Genetic Engineering and Biotechnology (KCGEB), UAE University, Al Ain, United Arab Emirates; [c]Department of Plant Science and Plant Genomics and Breeding Institute, Seoul National University, Seoul, Korea

ABSTRACT

In this study, transgenic *Arabidopsis* lines expressing a potato gene (*D43*), encoding Glyceraldehyde 3-phosphate dehydrogenase, were studied. The D43 plants exhibited improved morphological parameters and accumulation of photosynthetic pigments compared to wild-type (WT) plants under salinity stress conditions. In addition, the D43 transgenic plants showed significantly reduced electrolyte leakage, higher stomatal conductance, lower malondialdehyde (MDA) content, and higher proline content than the WT plants under salinity stress. The gene expression analysis showed that the D43 plants accumulated 1.7-fold, 2.2-fold, and 1.3-fold higher mRNA transcripts of genes encoding the antioxidant enzymes ascorbate peroxidase (APX), superoxide dismutase (SOD), and catalase (CAT), respectively under salt-stress conditions. Furthermore, they significantly altered the expression of seven major stress-responsive genes, which indicated that overexpression of the potato D43 gene gave salinity stress resistance to *Arabidopsis*. Chlorophyll-a fluorescence kinetics confirmed the efficient photon absorption, electron transport, and overall PSII efficiency that led to improved photosynthesis in the D43 plants subjected to NaCl-induced salinity stress. Overall, our findings have suggested that potato D43 is a potential candidate gene for developing salinity stress resistance in higher plants.

ARTICLE HISTORY
Received 28 March 2021
Accepted 24 July 2021

KEYWORDS
Abiotic stress; Arabidopsis; chlorophyll-a; GAPDH; photosystem II; reactive oxygen species; transgenic

1. Introduction

Glyceraldehyde-3-phosphate dehydrogenase (GAPDH) is a well-known enzyme involved in the glycolytic pathway, gluconeogenesis, and the Calvin cycle(Harper and Keeling 2003). Its primary function is to catalyze the NAD-dependent conversion ofglyceraldehyde-3-phosphate into 1,3-diphosphoglycerate. Evolutionarily, all eukaryotic glycolytic enzymes, including GAPDH, share a high similarity with eubacterial and archaebacterial homologs (Maeda and Fernie 2021). Photosynthetic eukaryotes have acquired two distinct forms of GAPDH, one cytosolic and one plastid-targeted (Harper and Keeling 2003), whereas, cytosolic GAPDH is involved in the conversion of glyceraldehyde3-phosphate into 1,3-bisphosphoglycerate. The plastid-targeted GAPDH plays a key role in photosynthetic CO_2 fixation (Cerff and Chambers 1979; Zhang et al. 2011).

Studies aimed at investigating the role of different forms of GAPDH in photosynthesis have revealed that accumulation of GAPDH can significantly affect the photosynthetic capacity of plants, as it plays an important role in the Calvin cycle (Calvin 1962; Heldt and Piechulla 2011). In recent times, overproduction of the chloroplast GAPDH has been reported to improve photosynthetic capacity under elevated CO_2 conditions in rice plants (Suzuki et al. 2021). Transgenic rice, with increased activity of chloroplast GAPDH, has shown a slight increase in biomass production along with significantly increased starch production, compared to the WT plants. Transcriptome analyses of *Arabidopsis* mutant plants, lacking a cytosolic GAPDH activity, have exhibited altered expression of genes involved in carbohydrate metabolism (Rius et al. 2006). Interestingly, increased levels of reactive oxygen species (ROS) and downregulation of several major glycolytic and photosynthetic genes has also been reported in the mutants, further indicating the critical involvement of cytosolic GAPDH in the major metabolic pathways of plants. Besides the well-known role of GAPDH in plant growth and development, several reports have indicated that GAPDH can play a vital role in abiotic stress tolerance. Reduced expression of GAPDH in tobacco plants, using a virus-induced, gene-silencing approach, demonstrated the critical role of GAPDH in drought tolerance (Kappachery et al. 2015). In another report, overexpression of a cytosolic GAPDH gene,*OsGAPC3,* was found to alleviate salt stress in rice plants (Zhang et al. 2011). Three isoforms of the *OsGAPC* genes were found to be responsive against multiple stresses including osmotic stress, heat, salinity, and methyl viologen-induced oxidative stress (Zhang et al. 2011).

Similar to other abiotic stresses, salinity stress in higher plants also leads to oxidative damage via ROS molecules, such as hydrogen peroxide (Ahanger et al. 2020). Plants have developed an efficient antioxidant machinery to remove the ROS molecules. Environmental stress conditions lead to

CONTACT Mayank Anand Gururani gururani@uaeu.ac.ae
*These authors contributed equally to this study.
Supplemental data for this article can be accessed https://doi.org/10.1080/17429145.2021.1962420
© 2021 The Author(s). Published by Informa UK Limited, trading as Taylor & Francis Group
This is an Open Access article distributed under the terms of the Creative Commons Attribution License (http://creativecommons.org/licenses/by/4.0/), which permits unrestricted use, distribution, and reproduction in any medium, provided the original work is properly cited.

photooxidation because of over-reduction of the photosynthetic electron transport chain (ETC), thus causing severe damage to the photosynthetic machinery of plants (Gururani et al. 2015). The ROS causes damage to proteins, DNA, and lipids, which ultimately affects the cellular functioning of plants. Under stress conditions, redox homeostasis is maintained by two arms of the antioxidant machinery the enzymatic components consisting of, ascorbate peroxidase (APX), superoxide dismutase (SOD), guaiacol peroxidase (GPX), glutathione-S-transferase (GST), and catalase (CAT); and the non-enzymatic compounds, such as, ascorbic acid (AA), reduced glutathione (GSH), α-tocopherol, carotenoids, phenolics, flavonoids, and proline (Khaliq et al. 2015; Alam et al. 2019). Photosystem II (PSII) is a key component of the photosynthetic machinery that encounters the impact of abiotic stress. In addition to the generation of ROS, abiotic stresses damage the photosynthetic apparatus, particularly PSII, due to an imbalance in the photosynthetic redox signaling pathways and the inhibition of PSII repair, leading to photoinhibition (Nath et al. 2013; Gururani et al. 2015). Plants have several mechanisms to overcome this problem, for example, reducing the rate of electron transport, by converting the excessively absorbed light into thermal energy (Takahashi and Badger 2011). Fast chlorophyll-a (Chl-a) transient kinetics can determine the PSII efficiency under normal and stress conditions. The analysis of Chl-a transients has the ability to detect interesting details related to the adjustment and alteration of the photosynthetic machinery during stress conditions (Goltsev et al. 2012; Kalaji et al. 2016).

In a previous study, several potential stress-associated candidate genes in *Solanum tuberosum* were identified using a large-scale yeast functional screening approach (Kappachery et al. 2013). Based on the relative tolerance to different stresses, 12 genes were reported to be the most effective in ameliorating the stress of drought and high survival rates in salinity, and high temperature stresses. One of the 12 identified genes, the cytosolic GAPDH, *StD43* (hereafter, *D43*), exhibited high tolerance levels under drought salinity and high temperature stress. This study was based on a hypothesis that overexpression of the *S. tuberosum D43* gene might promote salinity stress tolerance in *A. thaliana* through an improved photosynthetic performance. Transgenic *A. thaliana* plants expressing *D43* were subjected to salinity stress and the plants were evaluated for their putative stress tolerance by performing physiological assays and Chl-a transient kinetic analyses.

2. Materials and methods

2.1. Identification and sequence analysis of d43

The amino acid sequence of *S. tuberosum* (NCBI Acc. no. AFX67011), reported earlier, (Kappachery et al. 2013), was downloaded and analyzed. Phylogenetic analysis was done by using the National Center for Biotechnology Information (NCBI) Basic Local Alignment Search Tool (BLAST) pairwise alignments. Multiple sequence alignment (MultAlin) (Corpet 1988) was used for multiple sequence alignment, to compare and identify the differences between other *GAPDH* sequences in *S. tuberosum*. Subcellular localization of the D43 amino acid sequence was performed using the WoLF PSORT Prediction (https://www.genscript.com/tools/wolf-psort).

2.2. Arabidopsis transformation

The *D43* gene, which was cloned in the pMDC32 construct (Kappachery et al. 2015) was introduced into the *Agrobacterium tumefaciens* strain GV3101. Transgenic *Arabidopsis* lines were developed by using the floral dip method (Zhang et al. 2006). Positive transgenic *Arabidopsis* plants were selected using hygromycin (50μg/ml) plates and confirmed by the polymerase chain reaction (PCR), using gene-specific and CamV35S primers (Table 1). Positive transgenic D43 *Arabidopsis* plants from the T_1, T_2, and T_3 lines were confirmed by genomic DNA PCR using the *D43* gene specific primers (Table 1). T_3 generation was used for further experiments.

2.3. Stress treatments and determination of morphological parameters and pigment accumulation

Arabidopsis thaliana (both WT and transgenic D43 of the Columbia ecotype) were grown in soil in a plant growth chamber, at 22–24°C, with a 16-hour light/8-hour dark photoperiod. Four-week-old WT and T3-transgenic *Arabidopsis* plants were used for the study. For salt-stress treatments, 200 mM NaCl solution was used and the plants (WT-NaCl and D43-NaCl) were kept in a container with capillarity uptake for three days as described earlier (Brini et al. 2007). Plants watered with tap water served as controls (WT-NS and D43-NS). Plant height, root length, and number of leaves per plant were recorded and analyzed. In addition, the fresh weight of each plant was measured after subjecting the plant to salt-stress (Table 2).

2.4. Stomatal conductance, electrolyte leakage, and malondialdehyde (MDA) measurements

Stomatal conductance on the surface of the upper leaves was measured using a diffusion leaf porometer (SC-1; Decagon Devices, Inc., Pullman, WA, USA). All measurements were

Table 1. Description of the gene-specific oligo primers used in the study.

No.	Gene name	Oligo name	5′- Sequence -3′
1	Actin (Housekeeping gene)	AtACTrtF	CCGGTATTGTGCTGGATTCT
		AtACTrtF	TTCTCGATGGAAGAGCTGGT
2	Ascorbate peroxidase (APX)	AtAPXrtF	TGCCACAAGGATAGGTCTGG
		AtAPXrtR	CCTTCCTTCTCTCCGCTCAA
3	Superoxide dismutase (SOD)	AtSODrtF	TCCATGCAGACCCTGATGAC
		AtSODrtR	CCTGGAGACCAATGATGCC
4	Catalase (CAT)	AtCATrtF	AAGTGCTTCATCGGGAAGGA
		AtCATrtF	CTTCAACAAAACGCTTCACGA
5	pMDC-35S Promoter	pMD35S-F	GCACGACACACTTGTCTACT
		pMD35S-R	CGAGGAGGTTTCCGGATATTA
6	Delta1 pyrroline5-carboxylate synthase 1 (P5CS1)	AtP5CS1_rtF	GCAGCTTTGCGGATCTTCAG
		AtP5CS1_rtR	AAGTTGAGCTGCCGTCACAT
7	C2-domain ABA-related proteins (CAR9)	AtCAR9_rtF	GCATCACTTGGAGCAATGGG
		AtCAR9_rtR	TCGGCATCCATGGTGTCTTC
8	Rac-like GTP-binding protein (RAC7)	AtRAC7_rtF	TATGGGACACTGCCGGTCAA
		AtRAC7_rtR	ACCGACGAAGTTCAGGCATC
9	Enhanced EM Level bZIP12 transcription factor (EEL)	AtEELrtF	TGAGGAAGGGCTTGTTCGTC
		AtEEL_rtR	ACCGAGTGTAGGCTGCTTATG
10	Late embryogenesis abundant protein 7 (LEA7)	AtLEA7_rtF	ACGATGGGGGACAAAACACA
		AtLEA7_rtR	CGTTTGTGCAGCTTGAGACG
11	Lipid tansfer protein 3 (LTP3)	AtLTP3_rtF	TGGCTCCATGTGCAACCTAT
		AtLTP3_rtR	GAAATGCTCTTCGCAGTGGAC
12	Annexin 1 (AnnAT1)	AnnAT1_rtF	AACCGCTTTTGAAGGATGGG
		AnnAT1_rtR	GTCTTCGCCGTAGGTTTCGT

Table 2. Estimation of morphological parameters and pigment content in *Arabidopsis* plants exposed to salt-induced stress.

Parameter	WT-NS	WT-NaCl	D43-NS	D43-NaCl
Plant height (cm)	12.95 ± 0.29^{a}	9.82 ± 0.26^{b}	13.5 ± 0.35^{a}	11.6 ± 0.28^{c}
Root length (cm)	6.75 ± 0.19^{a}	2.74 ± 0.20^{b}	7.23 ± 0.21^{a}	4.16 ± 0.18^{c}
Leaves/plant	13.13 ± 0.36^{a}	12.26 ± 0.46^{a}	13.2 ± 0.43^{a}	12.66 ± 0.52^{a}
Fresh weight (g)	12.59 ± 0.28^{a}	8.84 ± 0.24^{b}	14.34 ± 0.25^{c}	11.07 ± 0.29^{d}
Chl A (mg/gdwb)	2.88 ± 0.17^{a}	0.84 ± 0.09^{b}	2.94 ± 0.13^{a}	1.07 ± 0.04^{c}
Chl B (mg/gdwb)	1.20 ± 0.45^{a}	1.07 ± 0.15^{a}	1.23 ± 0.27^{a}	1.49 ± 0.06^{a}
Total Chl (mg/g dwb)	4.08 ± 0.31^{a}	1.91 ± 0.08^{b}	4.16 ± 0.31^{a}	2.57 ± 0.05^{b}
Carotenoids (mg/g dwb)	0.59 ± 0.14^{a}	0.13 ± 0.06^{b}	0.52 ± 0.13^{a}	0.34 ± 0.05^{a}

Note: WT-NS, well-watered wild-type *Arabidopsis* plants; WT-NaCl, wild-type *Arabidopsis* plants exposed to salt stress (induced by 200 mM NaCl) for three days; D43-NS, well-watered transgenic *Arabidopsis* plants; D43-NaCl, transgenic *Arabidopsis* plants exposed to salt stress (induced by 200 mM NaCl) for three days; dwb-dry weight basis; Values represented in the table are the mean ± SEM from three independent assays with five replicates for each treatment. Different letters in a column are significantly different ($p \leq 0.05$) after Tukey's test (n = 5).

done at 25 ± 1°C and 55 ± 5% relative humidity, after calibrating the porometer. To measure electrolyte leakage, the leaf disks were suspended in 10 mL distilled water in a test tube and boiled. Then, the boiled filtrate was collected, and the electrical conductivity (ECa) was measured. Furthermore, the filtrate was brought to room temperature and was heated at 55°C for 30 min and the electrical conductivity (ECb) was recorded. The filtrate was then again boiled at 100°C for 10 min, and the electrical conductivity (ECc) was recorded. The electrolyte leakage was calculated using the formula, Electrolyte leakage (%) = (ECb - ECa / ECc) × 100.

To measure the MDA equivalent content, 500 mg of the leaf tissue sample was ground to a fine powder using liquid nitrogen and was homogenized in 5 mL of 50 mM buffer (0.07% $NaH_2PO_4{\cdot}2H_2O$ and 1.6% $Na_2HPO_4{\cdot}12H_2O$). The sample was centrifuged at 13,000 rpm and 4°C for 25 min and the supernatant was collected. Then, 4 mL of 20% trichloroacetic acid containing 0.5% thiobarbituric acid was added to 1 mL of the supernatant and was incubated at 95° C for 30 min, followed by keeping on ice for 10 min. The reaction mixture was again centrifuged at 13,000 rpm for 10 min, and the absorbance at 532 nm was recorded. The non-specific absorption at 600 nm was subtracted from the absorbance reading at 532 nm. The final MDA equivalent content was calculated as described earlier (Fu and Huang 2001).

2.5. Estimation of proline levels

Proline estimation through colorimetric analysis was carried out with the leaf samples taken from WT-NS, D43-NS, WT-NaCl, and D43-NaCl plants, subjected to salt-stress as described earlier(Gururani et al. 2015). About 500 mg leaf sample was ground in 10 mL of 3% aqueous sulfosalicylic acid. Equal volumes of the filtered homogenate were mixed in acid-ninhydrin and glacial acetic acid and allowed to react for 1 h. The reaction was then ceased by transferring the tubes onto ice and the chromophore-containing phase was extracted by using 4 mL of toluene. The absorbance of the extracted phase at 520 nm was measured. A standard curve was used to determine proline concentration in µmol g^{-1} FW.

2.6. Expression analysis of the genes encoding ROS-scavenging enzymes and salinity stress-responsive genes

The leaf samples were collected after salt stress and stored at −80°C until the start of the experiment. The expression of the three ROS-Scavenging enzymes APX, SOD, and CAT, from the stress and control samples, was performed through quantitative Real Time Polymerase Chain Reaction (qRT-PCR). In addition, the expression analysis of seven randomly selected salinity stress-responsive genes (listed in Table 1) was performed. Total RNA from the frozen *Arabidopsis* rosette was extracted using the Plant RNA Extraction Kit (NorgenBiotek, Canada). The cDNA was synthesized using the TruScript First Strand CDNA synthesis Kit (NorgenBiotek, Canada). The cDNA samples were diluted 10x on the QuantStudio5 System and SYBR™ Green PCR Master Mix (Applied Biosystem, USA), before using them as templates for qRT-PCR. The primers were designed using the PRIMER3 program and are listed in the Table 1. Actin was used as the internal control. The qRT-PCR program consisted of one cycle at 95°C for 3 min, followed by 35 cycles of 94°C for 30 s, 58°C for 15 s, and 72°C for 30 s, and a final cycle at 72°C for 5 min. The relative gene expression was determined as described earlier (Ghosh et al. 2017).

2.7. Chlorophyll a (Chla) fluorescence measurements

The chlorophyll *a* fluorescence transient in the leaves of the WT-NS, D43-NS, WT-NaCl, and D43-NaCl plants was measured using a PocketPEA (PlantEfficiencyAnalyzer, Hansatech, UK). The leaves of these plants were kept in the dark for at least 1 h, in the provided clips. The plotted fluorescence values were the mean of the three replicates per plant, recorded from the middle part of the fully developed leaves. The fluorescence transients were induced by one 650 nm red diode with 3000 µmol photons s^{-1} m^{-2}. The quantum yield of PSII photochemistry, Fv/FM ratio was calculated by the maximal fluorescence (F_M) and the minimal fluorescence (F_O) of the sampled leaves. The data was analyzed using the JIP-test equations in the Biolyzer software program (http://www.fluoromatics.com/biolyzer_software-1.php). The JIP-test equations were based on the Theory of Energy Fluxes in Biomembranes [21], which supported the general derivation of the actual quantum yield of primary photochemistry, $\phi_{Px} = TR_x/ ABS = 1 - F_x/F_M$, according to Paillotin [22]. The equations showcased that each energy flux of the energy cascade from the photon absorption flux (ABS) was converted into a free energy flux (RE), and finally stored by reduction of the end-electron acceptors of PSI. The definitions and formulae of the JIP-tests are expressed in the supplementary Table S1. As an effect of the salt-induced osmotic stress, the energy pipeline leaf model of the phenomenological fluxes was deduced using a Biolyzer. This energy pipeline model reveals the details on the efficiency of the flow of energy to the

photosynthetic electron transport chain components, through the PSII reaction centers (RCs), from the antennae. The arrow areas for each of the parameters, TR0/CS0, ABS/CS0, ET0/CS0, and DI0/CS0, exhibit the efficiency of trapping, light absorption, electron transport, and dissipation per cross-section of PSII, respectively, (Varghese et al. 2019; O. Alyammahi and Gururani 2020), in the control and transgenic plants exposed to salt-stress.

2.8. Statistical analysis

Three replicates were used in all experiments and the experiments were repeated at least three times. The data obtained was analyzed using Origin 8.1 (www.originlab.com) and the statistical differences were obtained using one-way ANOVA followed by Tukey's multiple comparison tests.

3. Results

3.1. Analysis of *D43* from *S.* tuberosum

The analysis of *S. tuberosum* D43 amino acid sequence using InterProScan (http://www.ebi.ac.uk/InterProScan/) revealed that this protein of 337 amino acids has a NAD-binding domain of 150 amino acids (denoted by red in Figure 1), a Glyceraldehyde 3-phosphate dehydrogenase active site of 7 amino acids (denoted by green in Figure 1), and a C-terminal catalytic domain of 157 amino acids (denoted by black in Figure 1). For phylogenetic analysis, the amino acid sequence of D43 was aligned with 12 other GAPDH proteins from potato and it exhibited a high similarity with all the homologs.

3.2. Generation of transgenic Arabidopsis *plants*

For overexpression of *D43* in *Arabidopsis,* the full-length cDNA (NCBI Acc. JX845304) encoding the *S. tuberosum D43* gene was cloned in the pMDC32 vector (Figure 2A) and mobilized to *Agrobacterium* GV3101, as described earlier (Kappachery et al. 2015). PCR and RealTime qPCR confirmed the presence of the *D43* gene in the T3 transgenic *Arabidopsis* plants, whereas, the presence of *D43* was not detected in the WT plants (Figure 2B, C).

3.3. Assessment of morphological and biochemical changes

The morphological parameters like plant height, root length, and number of leaves on plants subjected to salt-stress were recorded (Table 2). As expected, the WT–NS and D43-NSplants exhibited an increase in average plant height, leaves/plant, and fresh weight compared to that of WT-NaCl and D43-NaCl plants. However, there was a notable difference in root length among the control and stressed plants. The D43-NaCl plants showed a significantly higher average plant height, root length, and fresh weight than the WT-NaCl plants. The average number of leaves/plant was not significantly different in the WT-NaCl and D43-NaClplants, although visibly, the D43-NaCl leaves appeared greener than those on the WT-NaCl plants (data not shown). The chlorophyll estimation in WT and D43 plants further showed the difference in the physiological state of these plants. After three days of salt-induced stress, the chlorophyll content in the leaves of D43-NS was recorded as being the highest, and simultaneously, WT-NaCl recorded the lowest levels of chlorophyll. Interestingly, the levels of chlorophyll in the D43-NaCl plants exhibited 25.6% higher accumulation of chlorophyll than that in the WT-NaCl plants. A similar trend in the reduced accumulation of carotenoids was noted in the WT and D43 plants exposed to salinity stress. Although the WT plants showed almost 78% reduced accumulation of carotenoids after three days of salinity stress, the D43 plants recorded only 34.6% reduced carotenoid accumulation (Table 2).

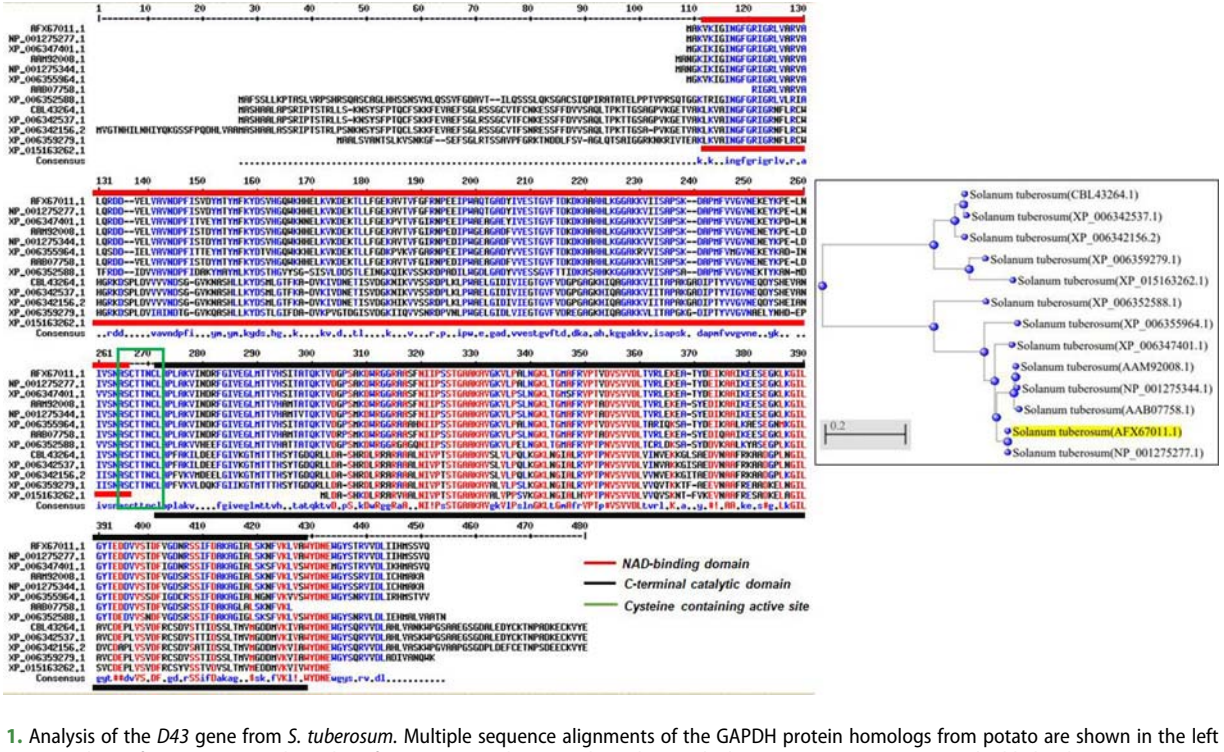

Figure 1. Analysis of the *D43* gene from *S. tuberosum.* Multiple sequence alignments of the GAPDH protein homologs from potato are shown in the left panel. Phylogenetic analysis of GAPDH protein homologs from potato is shown in the right panel. The *D43* gene (AFX67011.1) is highlighted.

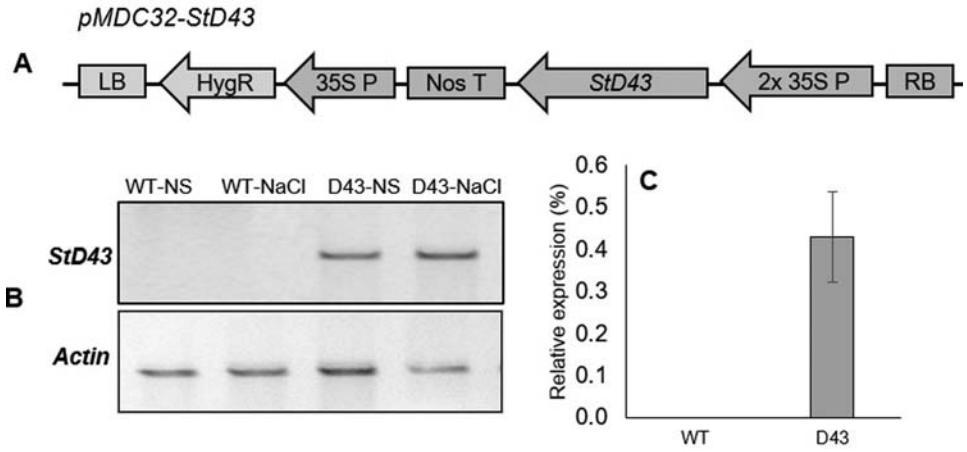

Figure 2. Overexpression of *D43* intransgenic *Arabidopsis* plants and validation of transgenics. (A) Schematic diagram of the T-DNA region of the pMDC32 construct expressing the *D43* gene under the control of the 35S-promoter, which was used for *Arabidopsis* transformation (B) RT-PCR analysis of *D43* transgenic lines. (C) qRT-PCR analysis of transgenic *Arabidopsis* plants expressing potato *D43* gene. Error bars indicate mean ± SEM from three independent assays with five replicates for each treatment.

3.4. Estimation of electrolyte leakage, stomatal conductance, malondialdehyde, and proline content

There was no significant difference in electrolyte leakage between the WT-NS and D43-NS plants, however, a significant increase (107.8%) in electrolyte leakage was recorded in WT compared to a 66% increase in D43 plants after three days of salinity stress (Figure 3A). The average values of stomatal conductance in the WT-NS plants were similar to that of D43-NS. Besides, among the stressed plants, the D43-NaCl plants showed a 38.5% reduction in stomatal conductance compared to the 61.1% reduction in the WT-NaCl plants (Figure 3B). The MDA equivalent contents determined the effect of salinity stress on membrane lipid peroxidation. The D43-NaCl plants exhibited almost a similar range in MDA equivalent values as the control plants, such as, WT-NS and D43-NS, however, the value was recorded as 48.1% lower in D43-NaCl compared to the WT-NaCl plants (Figure 3C).

Accumulation of the osmoprotectant molecule proline, is an important indicator of stress tolerance in higher plants. The D43 plants showed a 60.3% increased proline concentration, even as a 42.2% increase in proline was recorded in WT plants after a three-day salinity stress treatment (Figure 3D). This indicates the significance of proline in plant stress tolerance and the significantly higher accumulation of proline in D43 plants, attributed to their salt stress tolerance.

3.5. Overexpression of StD43 induces expression of antioxidant enzymes and stress-responsive genes under salinity stress

qRT-PCR analysis on the WT and D43 *Arabidopsis* plants under stress conditions, revealed that the expression level of ROS-scavenging enzyme genes, APX, SOD, and CAT genes, was higher in the transgenic stressed plants, that is, the D43-NaCl plants (Figure 4). This, in turn, indicated that these plants showed the highest level of tolerance towards radicals produced by salt-stress. To evaluate the salinity stress tolerance in D43 plants, seven stress-responsive genes were selected for gene expression analysis. The expression of a C2-domain ABA-related gene (*CAR9*) involved in regulating the sensitivity to abscisic acid (Qin et al. 2019) was significantly higher in WT plants, as compared to that in the D43 plants exposed to salt stress. Expression of pyrroline-5-carboxylate synthetase 1 (*P5CS1*), an enzyme related to proline biosynthesis (Varghese et al. 2019), was significantly higher in D43 plants under salinity stress, compared to WT plants. *EEL*, a transcription factor involved in ABA biosynthesis (Lindemose et al. 2013) also showed increased expression in WT and D43 plants exposed to salt stress, however, the increase in *EEL* gene expression noted in the D43-NaCl plants was remarkably higher in the WT-NaCl plants. The *RAC7* gene encodes a GTPase protein involved in signal transduction during abiotic stress in plants (Huang et al. 2019). The expression of *RAC7* was approximately two-fold higher in D43-NaCl compared to WT-NaCl plants. The D43 plants showed a 2.6-fold higher *LEA7* gene expression in D43 plants compared to WT plants subjected to salt stress. It is a well-known fact that late embryogenesis-abundant (LEA) proteins played a significant role in the growth, development, and abiotic stress tolerance in plants (Chen et al. 2019). The gene encoding for lipid transfer protein 3 (*LTP3*) played a crucial role in abiotic stress signaling (Pan et al. 2016). D43-NaCl plants recorded a 3.6-fold higher expression of *LTP3* compared to WT-NaCl plants. The *AnnAt1* gene encoded for a protein belonging to the Annexin multigene family, was known to regulate various cellular processes, growth, development, and abiotic stress tolerance in plants (Cantero et al. 2006). Similar to the other seven stress-responsive genes selected for this study, the expression of *AnnAt1* was significantly higher in D43 plants compared to WT plants, under salt stress conditions (Figure 4).

3.6. Transgenic D43 plants were more photosynthetically active under salt-stress condition

To estimate the photosynthetic efficiency of the control and transgenic *Arabidopsis* plants exposed to salt stress, the Chl-a fluorescence JIP-test was used. Fluorescence transients of dark-adapted leaves of WT and D43 plants under NS and NaCl stress conditions are shown on a logarithmic scale from 20 μs to 1 s in Figure 5(A). A typical OJIP shape was found in all the samples with distinct maximum variable fluorescence ($F_M - F_0 = F_V$), indicating that all plants were photosynthetically active. However, a significant reduction in the slope was observed in WT-NaCl plants, illustrating

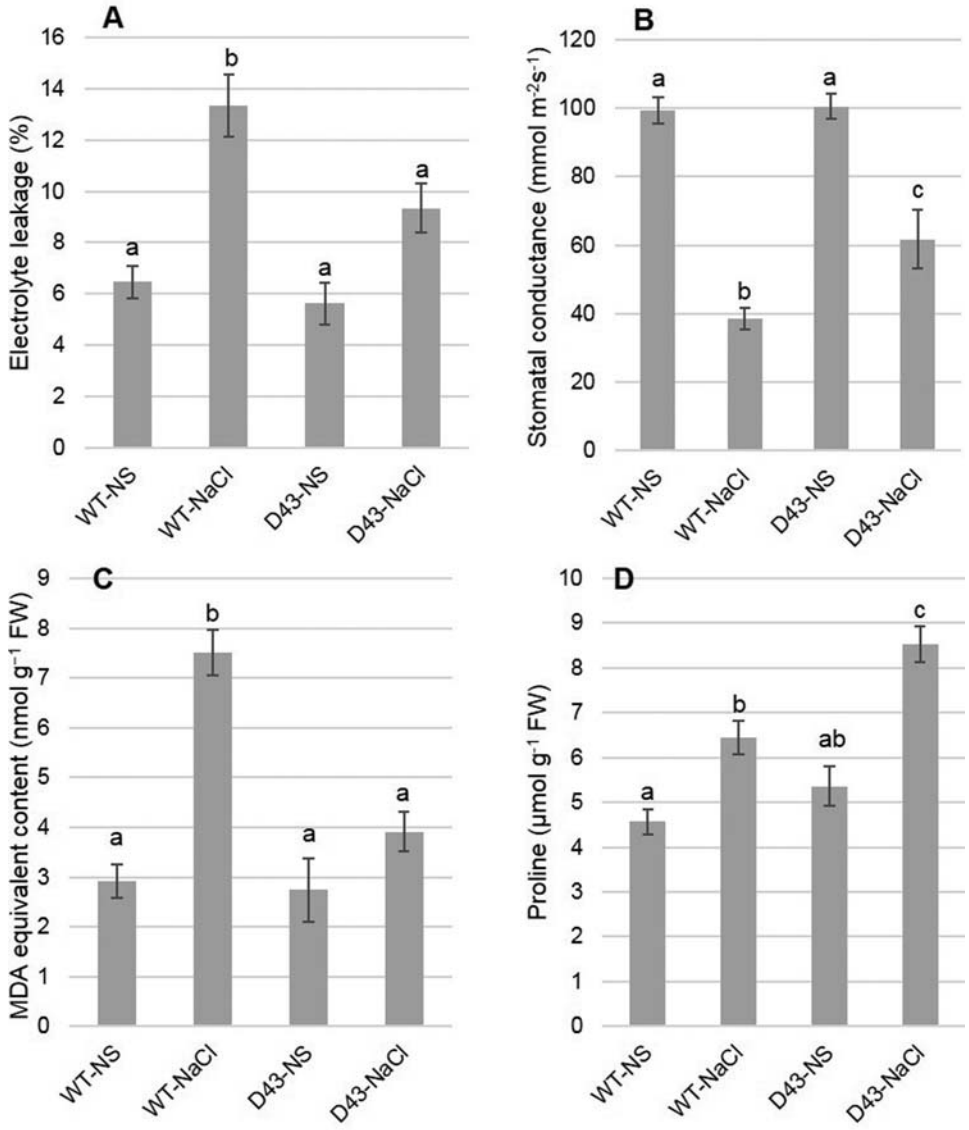

Figure 3. Biophysiological responses of D43 transgenic *Arabidopsis* plants.(A) Percent of electrolyte leakage, (B) Stomatal Conductance (mmol $m^{-2}s^{-1}$), (C) MDA equivalent content (nmol g^{-1} FW), and (D) Proline. WT-NS, well-watered wild-type *Arabidopsis* plants; WT-NaCl, wild-type *Arabidopsis* plants exposed to salt stress (induced by 200 mM NaCl) for three days; D43-NS, well-watered transgenic *Arabidopsis* plants; D43-NaCl, transgenic *Arabidopsis* plants exposed to salt stress (induced by 200 mM NaCl) for three days; Values represented are the mean ± SEM from three independent assays with five replicates for each treatment. Different letters in a column are significantly different ($p \leq 0.05$) after Tukey's test ($n = 5$).

that this group was more susceptible to stress-related damage during photosynthesis, compared to the D43-NaCl group. Subsequently, the maximum photochemical efficiency of photosystem II (F_v/F_m) as well as the performance index (PI) were recorded. The F_v/F_m ratios of the samples were used to determine the photo inhibitory effects on the electron transport system due to stress conditions, even as the PI value provided the fluorescent changes in antenna conformation and energy fluctuation. The F_v/F_m ratios were in the range of 0.81–0.83 for the control plants, while it ranged from 0.73–0.77 for the plants exposed to salt stress (Figure 5B). Interestingly, the value of the F_v/F_m ratio showed an increase in D43-NaCl plants, as compared to the WT-NS plants, indicating that transgenic plants overexpressing the *D43* gene could sustain the aforementioned stress condition when compared with the control plants (Figure 5B).

A similar indication was also obtained from the PI values of the D43-NaCl plants, having a higher value than the WT-NS plants. The PI value of the D43-NaCl plants was higher than that of WT-NS under stress conditions (Figure 5C). The PI value of both the controls (WT-NS and D43-NS) had a similar range, even as the PI value of the WT-NaCl recorded the lowest. Although there was no significant difference in the average PI value of WT-NS and D43-NS, the average PI value of WT-NaCl plants was 37% lower than the D43-NaCl plants.

The JIP-analyses of the WT and D43 *Arabidopsis* plants, under normal and salt stress conditions, further revealed that overexpression of D43 in *Arabidopsis* significantly increased the absorption flux of photons per active RCs when these plants were subjected to salt-stress conditions (Figure 5D). A marked decrease in absorption (ABS), trapping (TRo), and electron transport (ETo) per RC in the WT-NaCl plants compared to the D43-NaCl plants indicated that the NaCl-induced salinity stress decreased the electron transport, probably because of an increase in the number of inactive PSII RCs.

The parameter Fv/Fo represented the concurrent alterations in Fv and Fo, which determined the overall PSII quantum yield efficiency (Kumar et al. 2020). WT plants showed a

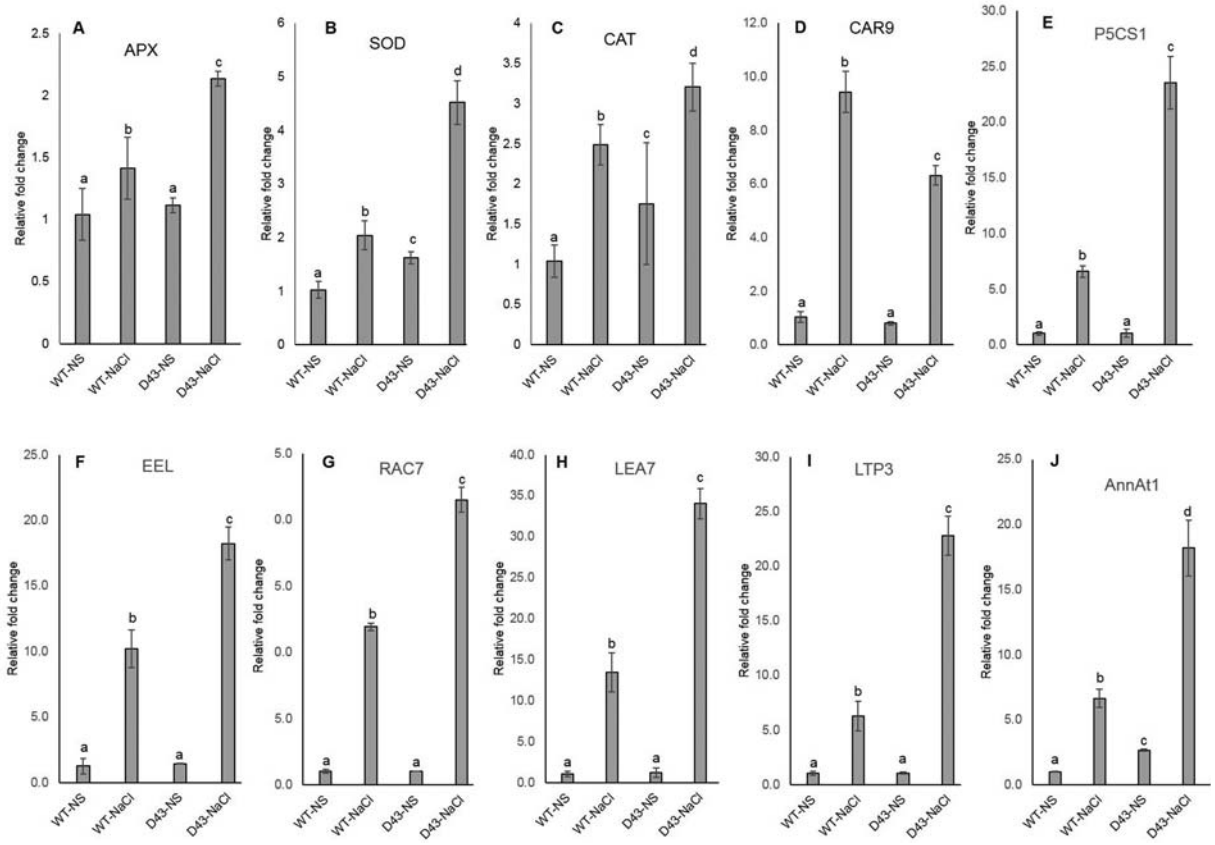

Figure 4. Relative expression fold change of the stress-responsive genes. (A) Expression analysis of Antioxidant genes. (B) Expression analysis of seven stress responsive genes (*CAR9, EEL, LTP3, RAC7, AnnAt1, P5CS1, and LEA7*). Fold expression values are normalized with Actin internal control; WT-NS, well-watered wild-type *Arabidopsis* plants; WT-NaCl, wild-type *Arabidopsis* plants exposed to salt stress (induced by 200 mM NaCl) for three days; D43-NS, well-watered transgenic *Arabidopsis* plants; D43-NaCl, transgenic *Arabidopsis* plants exposed to salt stress (induced by 200 mM NaCl) for three days; Values represented in the table are the mean ± SEM from three independent assays with five replicates for each treatment. Different letters in a column are significantly different ($p \leq 0.05$) after Tukey's test ($n = 5$).

significantly reduced Fv/Fo under salinity stress compared to the D43 plants, indicating a reduced electron transport in these plants.

The quantum yields of primary photochemistry (φPo), electron transport (φEo), and the efficiency/per trapped excitation (Ψo) were consistently affected in WT plants under salinity stress compared to D43 plants. These parameters provided precise details on electron transport movement at the PSII acceptor sites (Strasser et al. 1995).

The parameter Area and Sm, respectively, expressed the complementary area between the fluorescence induction curve and Fm, and the complementary area of the plastoquinone (PQ) pool between PSII and PSI. These values were consistently less in WT plants as compared to the D43 plants subjected to salinity stress conditions (Figure 5D).

The parameters Vi and Vj that reflected the relative variable fluorescence at the I and J-steps of OJIP transient, respectively (Xiao et al. 2020), was significantly increased in the WT-NaCl plants, indicating a negatively affected electron transport at the donor side of PSII.

Although, the ABS/CS0 parameter that describes the number of photons absorbed by the antenna molecules was high in the NT-NS and D43-NaCl plants, a decrease in ABS/CS0 was observed in the NT-NaCl plants when compared with the D43-NaCl plants, indicating a decline in the energy absorbed per excited cross-section (Figure 5E).

The parameter ET0/CS0, that indicated the photosynthetic electron transport in a PSII cross-section and the rate at which QA was reoxidized over a cross-section of active RCs, was recorded, evidently higher in D43-NaCl plants, as compared to the NT-NaCl plants. This revealed that the PSII-RCs were activated and that the PSII-donor side was less affected in D43-NaCl plants than in the WT-NaCl plants.

The parameter DI0/CS0, indicated that the total dissipation measured over the cross-section of the samples that contained inactive and active RCs. A decrease in the density of active RCs (Figure 5, open circles) and an increase in the density of inactive RCs (Figure 5, dark circles) were observed in both WT-NaCl and D43-NaCl plants under stress.

4. Discussion

GAPDH is considered as one of the housekeeping enzymes that has an imperative role in glycolytic energy metabolism (Muñoz-Bertomeu et al. 2010). Conventionally, it has been used as a model protein for protein structure analysis and as an internal control for relative gene expression analysis. However, a study in plants revealed that GAPDH displayed exceptionally high expression variability, limiting its use as an internal control (Jain et al. 2006). Studies in rice, *Arabidopsis,* and potato revealed the significant role of GAPDH in abiotic stress physiology. A previous study identified a stress-responsive potato GAPDH gene (*D43*), through yeast functional complementation, which could identify genes involved in drought tolerance (Kappachery et al. 2013), *D43* was further validated for its role in drought

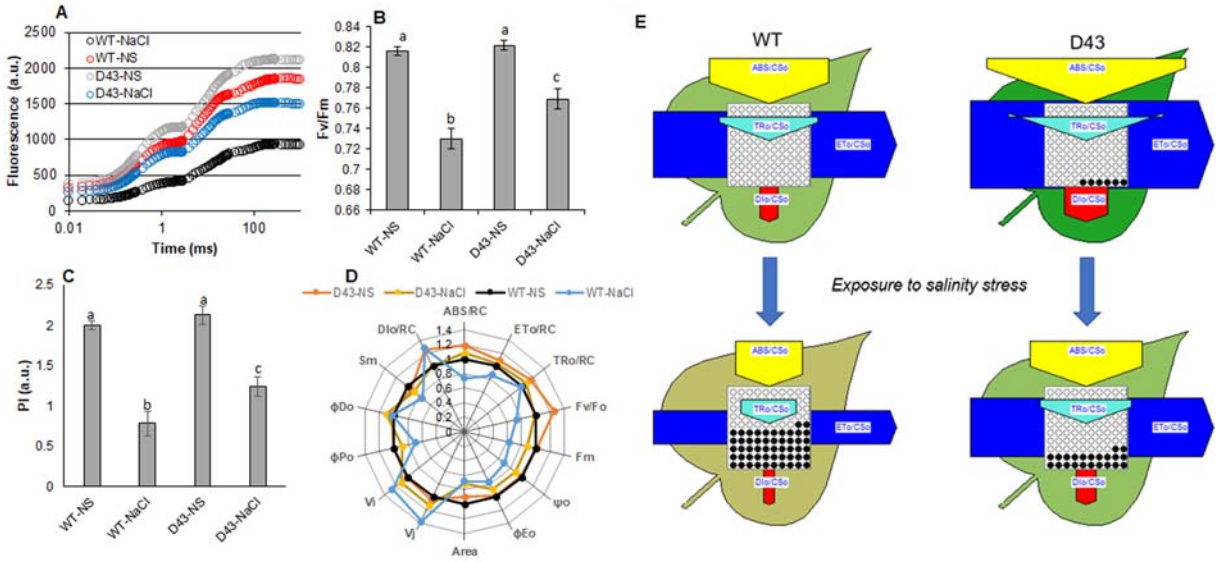

Figure 5. Photosynthetic performance of the D43 *Arabidopsis* transgenic plants. (A) Chlorophyll-a fluorescence kinetic OJIP of the *Arabidopsis* plants adapted to dark. Polyphasic curves of each line highlight the average of nine measurements (three measurements per plant, three different parts); (B) Estimation of photochemical efficiency (Fv/Fm); (C) performance index (PI);(D) Radar plot with a series of parameters derived from JIP-test analyses of the experimental fast OJIP transients. Notes: This plot exhibits putative differences in the structure and function of the photosynthetic apparatus under normal and salt stress conditions in *Arabidopsis* plants; (E) Energy pipeline leaf model of phenomenological fluxes (per cross-section, CSo) in wild-type *Arabidopsis* (WT-NS) and transgenic *Arabidopsis* plant (D43) leaves under normal (control) and salt stress conditions. The value of each parameter can be seen in the relative changes in width of each arrow. Active RCs are shown as open circles and inactive RCs as closed circles; WT-NS, well-watered wild-type *Arabidopsis* plants; WT-NaCl, wild-type *Arabidopsis* plants exposed to salt stress (induced by 200 mM NaCl) for three days; D43-NS, well-watered transgenic *Arabidopsis* plants; D43-NaCl, transgenic *Arabidopsis* plants exposed to salt stress (induced by 200 mM NaCl) for three days. Values represented in the table are the mean ± SEM from three independent assays with five replicates for each treatment. Different letters in a column are significantly different ($p \leq 0.05$) after Tukey's test ($n = 5$).

tolerance by generating and analyzing the transgenic D43 potato plants (Kappachery et al. 2015). Enhanced expression of the *StD43* gene in potato improved the ability of the plants for drought tolerance (Kappachery et al. 2015). Furthermore, it was revealed that altered expression of GAPDH under stress, facilitates the survival of plants under water-deficit stress (Kappachery et al. 2015). In this study, transgenic *Arabidopsis* plants expressing potato *D43* gene were developed and evaluated for their photosynthetic performance under salt stress.

The transgenic *Arabidopsis* plants with overexpressed *D43* gene (D43-NaCl) accumulated a higher amount of total chlorophyll content than the WT-NaCl plants, when exposed to salt-stress for three days (Table 2). The plants appeared greener with visible differences, especially in terms of growth between the D43 and WT plants. Reduced electrolyte leakage, increased stomatal conductance, lower MDA accumulation, and enhanced proline accumulation in D43-NaCl plants (Figure 3A–D) was in accordance with several previous findings (Sreenivasulu et al. 2000; Puyang et al. 2015; Alavilli et al. 2016; Blankenagel et al. 2018). A recent study on rice demonstrated that expression of the *OsGAPB* gene increased the CO_2 assimilation rate and chlorophyll content in rice subjected to low or light stress (Liu et al. 2020). Similarly, a recent study on melatonin-treated pepper plants demonstrated improved root and shoot biomass, higher accumulation of chlorophylls, and improved fruit yield (Kaya et al. 2020).

Earlier, reports had highlighted the role of proline in stabilizing the subcellular structures and detoxifying the free radicals, and hence, its accumulation is considered an indication of abiotic stress tolerance in plants at the metabolic level (Ahmad et al. 2010; Kong et al. 2015; Kohli et al. 2019). Increased accumulation of osmolytes such as proline has been associated with improved stress tolerance in plants. Moreover, it has been suggested that manipulation in the proline biosynthetic pathway induces abiotic stress tolerance in plants (Per et al. 2017). Recent studies on soybean plants treated with 24-epibrassinolide demonstrate increased accumulation of proline under salt stress, suggesting the protective role of proline in higher plants under stress (Alam et al. 2019). In this study, a significantly higher proline accumulation in the D43 plants was observed compared to that of WT plants exposed to salt-stress (Figure 3D), indicating the role of proline for stress tolerance and integrity of the plant cellular system for survival.

Stress-mediated decline in plant growth and photosynthesis has been documented in numerous studies (Ahanger et al. 2020; Onoud Alyammahi and Gururani 2020; Salim Akhter et al. 2021). Poor uptake of magnesium and nitrogen during salinity stress is considered as the primary cause of reduced chlorophyll accumulation in plants (Ahanger et al. 2020). Increased plant height, root length, and fresh weight in D43 plants compared to WT plants, implies that overexpression of the potato *D43* gene encoding for cytosolic GAPDH conferred notable salt-stress tolerance in *Arabidopsis* plants. Improved chlorophyll accumulation and agronomic parameters in sweet pepper (Abdelaal et al. 2020), barley (Salim Akhter et al. 2021), and soybean (Alam et al. 2019) plants under salinity stress have been reported recently.

Abiotic stresses lead to the formation of cellular ROS molecules like H_2O_2 and hydroxyl radicals (OH), which in turn cause lipid peroxidation of membranes (Khan et al. 2020). Moreover, these radicals can damage DNA, RNA, protein, and carbohydrates leading to cell death. The ROS scavenging enzymes such as APX, CAT, and SOD remove the free radicals produced during abiotic stress conditions in addition to their role of protecting the membranes and DNA from damage (Noctor et al. 2014; Hussain et al. 2018). In this

study, overexpression of the *D43* (GAPDH) gene upregulated the expression of CAT, APX, and SOD levels, indicating that GAPDH is involved in protecting the mechanism of the plant from salt stress (Figure 4A–C). Consistent with these results, overexpression of cytosolic GAPDH has been reported to exhibit improved tolerance against salinity stress in rice (Zhang et al. 2011). Furthermore, increased expression of *CatA* and other stress-responsive genes,*Lip9, RD29,* and *DREB2A* was observed in overexpressed transgenic rice plants (Zhang et al. 2011). Similar increased levels of expression of genes, encoding antioxidant enzymes APX, SOD, and CAT in response to abiotic stresses, have been reported in various crops (Zhang et al. 2015; Azarabadi et al. 2017; Salwa Akilan et al. 2019; Onoud Alyammahi and Gururani 2020).

To gain further insight into the mechanism of induced salt stress tolerance in D43 plants, the expression profile of seven stress-responsive genes was determined. The C2-domain ABA-related (CAR) proteins played vital roles in ABA signaling under abiotic stress conditions in plants (Qin et al. 2019). This protein was known to facilitate the interaction of ABA receptors with the plasma membrane, thereby regulating a sensitivity towards ABA (Rodriguez et al. 2014). Another study reported that *Arabidopsiscar9* mutants showed hyposensitivity to ABA (Qin et al. 2019). Overexpressing a homologous *CAR* family gene in rice was reported to induce tolerance against multiple stresses (Yokotani et al. 2009). In our results, we noted that although the expression of *CAR9* was enhanced in D43 plants when subjected to salinity stress, the WT plants also showed significantly higher expression of *CAR9* under salt stress conditions (Figure 4D). The possible reason for this significant difference in *CAR9* expression between WT-NaCl and D43-NaCl could be the altered expression of some other transcription factor or enzyme involved in the ABA biosynthetic pathway.

Increased endogenous proline content exerts abiotic stress tolerance (Gururani et al. 2013a; Varghese et al. 2019). This increased accumulation of proline in D43-NaCl (Figure 3D) must be accompanied with upregulation of the *P5CS1* gene. *P5CS1* catalyzes the conversion of L-glutamic acid to glutamate-5-semialdehyde and its overexpression has been reported to confer salinity stress tolerance in rice (Choudhary et al. 2005) and potato (Hmida-Sayari et al. 2005). We have observed a remarkably higher proline content accompanied by a 3.5-fold increase in the *P5CS1* transcript levels in D43-NaCl plants compared to WT-NaCl plants (Figure 4E), thus implicating that overexpression of *D43* improved the accumulation of proline during salinity stress, in transgenic *Arabidopsis D43* plants.

An enhanced EM Level bZIP12 transcription factor (EEL) is a transcription factor associated with ABA biosynthesis. EEL is known to antagonize an important ABA response locus, *ABI5* negatively regulates photosynthesis by activating chlorophyll degradation (Finkelstein 2010; Yoshida et al. 2014; Skubacz et al. 2016). Significantly, higher *EEL* expression in D43-NaCl thus confirms that damage to the photosynthetic apparatus and chlorophyll degradation was less severe in the D43 plants than in the WT, under salinity stress (Figure 4F).

RAC7 belongs to a plant-specific protein family of Rho GTPases that are involved in the regulation of plant growth, development, and abiotic stress responses (Fu et al. 2018). One of the proteins of this family, OsRac1, was reported to play a vital role in ROS production and cell death (Kawasaki et al. 1999). Although, the expression of *RAC7* was induced in both the WT and D43 lines, a significantly higher accumulation of mRNA transcripts was observed in the D43-NaCl plants, suggesting an efficient ROS machinery in these plants (Figure 4G).

LEA7 is a gene that encodes a protein of the Late embryogenesis-abundant (LEA) family known to regulate plant growth, development, and abiotic stress responses (Chen et al. 2019). The expression of *LEA* genes is regulated by ABA, a key phytohormone, involved primarily in the dehydration stress response. A 2.5-fold higher relative expression of *LEA7* in D43-NaCl plants, compared to that of WT-NaCl plants, (Figure 4H) clearly indicated that overexpression of *D43* promoted ABA-mediated salinity stress response in D43 plants.

Guo et al. (2013) reported that Lipid Transfer Protein 3 (LTP3) not only regulated the biotic stress response in plants, but also played a critical role in response to environmental stresses, such as, freezing and drought. Overexpression of *Zea mays LTP3* a homolog of *Arabidopsis LTP3,* led to improved salinity stress tolerance (Zou et al. 2013). Our results were in accordance with the previous findings, as we noticed a 3.6-fold higher expression of *LTP3* in the D43-NaCl plants compared to that in the WT-NaCl plants (Figure 4I).

Annexins belonged to a calcium-dependent, membrane-binding multigene family of proteins, with diverse functions. Previous findings confirmed that the mRNA levels of *Arabidopsis* Annexin (*AnnAt1*) were upregulated when the plants were exposed to different abiotic stresses (Konopka-Postupolska et al. 2009). Furthermore, the authors demonstrated that overexpression of AnnAt1 induced improved drought tolerance, whereas, knockout mutants showed increased sensitivity to drought in *Arabidopsis* plants. Our data suggested that D43 plants accumulated 2.7-fold higher mRNA transcript levels of *AnnAt1* than the WT plants subjected to NaCl-induced salinity stress (Figure 4J).

Over the years, the impact of abiotic stresses on the photosynthetic components has been evaluated using Chl-a fluorescence transient kinetics, which is comprised of four phases: O, the origin, P, the peak, and J–I, the intermediate phases (S. Akilan et al. 2019; Onoud Alyammahi and Gururani 2020). Analysis of the OJIP transients is a widely used technique to evaluate the response of PSII machinery against various stresses in higher plants (Oukarroum et al. 2012; Gururani et al. 2013a, 2013b; Zivcak et al. 2014; Zivcak et al. 2014; Choi et al. 2017; Ghosh et al. 2017). Exposure of WT and D43 plants to 200 mM NaCl greatly changed the OJIP transient curves (Figure 5A). However, the decline recorded in the polyphasic curve in D43 exposed to salt stress was notably less compared to that of WT plants. Previous reports that indicate a decline in the transient curves account for the inhibition of ETC at the PSII donor site and a decrease in the electron acceptor pool of PSII (Mathur et al. 2011; Gururani et al. 2015). The Fv/Fm ratio and PI, which express the photochemical efficiency of PSII and the vitality of plants under stress, are key indicators of the plants' overall physiology (Kalaji et al. 2016). The values of Fv/Fm and PI are significantly higher in the D43-NaCl plants than WT-NaCl plants, demonstrating a positive role of overexpression of *StD43* in *Arabidopsis* plants exposed to salinity

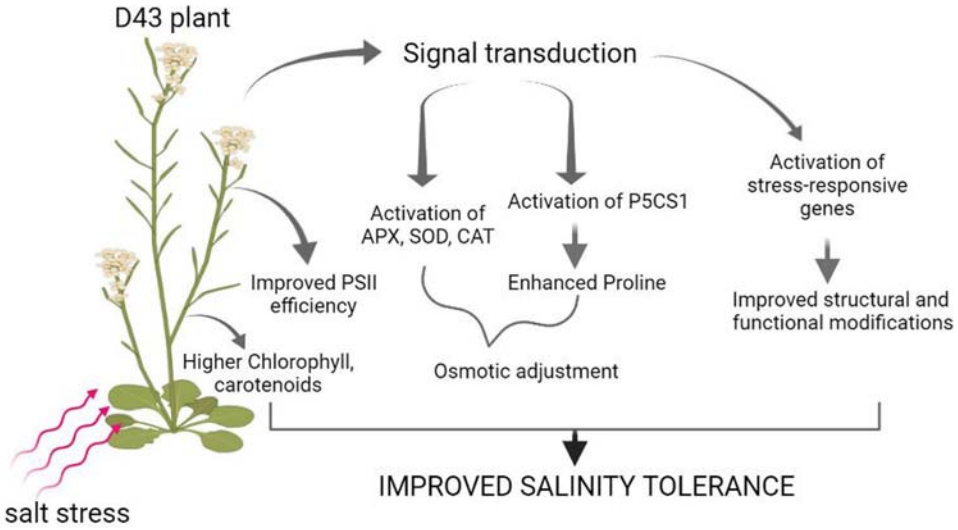

Figure 6. A hypothetical model explaining the possible mechanism of action underlying the induced salinity stress tolerance in D43 plants. The diagram was created in BioRender.com.

stress (Figure 5B,C). Similar findings in stress-tolerant plants have been reported in various crops, including rice (Kumar et al. 2017), oats (Varghese et al. 2019), pepper (Kaya et al. 2020), and barley (Salim Akhter et al. 2021), under salt stress conditions.

The analysis of OJIP transients not only assesses the negative impact on the PSII acceptor side, but also provides information on critical parameters ABS, TR, ET, and RE. The energy fluxes per RC (ABS/RC, ETo/RC, and TRo/RC) express the specific functional parameters (Figure 5D), while the energy fluxes per excited cross sections (ABS/CSo, ETo/CSo, TRo/CSo, and DIo/CSo) represent their comparable phenomenological energy fluxes. Previous studies have shown that salinity reduces the quantum yield of PSII electron transport, the energy available for the RCs, and the efficiency in the capability of PSII for oxygen evolution (Kalaji et al. 2011; Gupta 2020). The extrinsic PSII proteins protect the Mn-containing catalytic center that is involved in the oxygen evolution (Sasi et al. 2018). High salinity has been known to exert deleterious effects on these extrinsic PSII proteins, thereby, damaging the oxygen evolution efficiency of plants (De Las Rivas et al. 2007; Papageorgiou and Govindjee 2014).

The ratio Fv/Fo is considered as one of the most sensitive parameters of photosynthetic ETC, as it expresses the ability of electron donation from the PSII-catalytic center to its donor side (Fricke and Peters 2002). D43-NaCl plants showed significantly higher Fv/Fo ratio than the WT-NaCl plants, suggesting improved electron transport in these plants under salinity stress (Figure 5D). Soybean plants exposed to high concentration of Nickel were reported to show higher values of Fv / Fo when treated with jasmonic acid (Sirhindi et al. 2016). Similar findings were recently reported in barley plants exposed to different concentrations of salt (Salim Akhter et al. 2021).

The parameters Vi and Vj that express the variable fluorescence at the I and J phases of the polyphasic curve, have been attributed to the accumulation of Q_A and the plastoquinone pool, and the inability to pass the electrons to the Calvin cycle (Kalaji et al. 2014). Significantly lower values of Vi and Vj in the D43-NaCl plants indicated a more efficient ETC compared to the WT-NaCl (Figure 5D). These findings were in agreement with the previous reports (Mehta et al. 2010; Kalaji et al. 2014; Salim Akhter et al. 2021). The increase in Vi and Vj due to salinity stress led to a decrease in ETo/RC and ψ_0 (probably the trapped electron was transferred to ETC beyond Q_A) in WT and D43 plants. However, the D43 plants exhibited remarkably higher values of these parameters compared to WT, when exposed to salinity conditions. Similarly, the values of other quantum yields and efficiencies (ϕPo, ϕEo, ϕDo) were also recorded as being higher in D43-NaCl compared to WT-NaCl plants (Figure 5D). Similar results were observed in stress-tolerant plants (Yusuf et al. 2010; Kalaji et al. 2014; Vuletic and Spanic 2019; Onoud Alyammahi and Gururani 2020; Salim Akhter et al. 2021).

Another parameter that represented the area between the Fo and Fm steps was an indicator of electron transport to the plastoquinone pool. A lower area in the D43-NaCl plants suggested a reduction in the electron transport from RC to plastoquinone pool. Several previous reports have documented similar findings in different plants under various abiotic stress conditions (Mehta et al. 2010; Mathur et al. 2011; Kalaji et al. 2012; Salim Akhter et al. 2021).

The average values of the ABS/CSo, TRo/CSo, ETo/CSo, and DIo/CSo were markedly higher in the D43-NaCl plants compared to those of the WT-NaCl plants, indicating that overexpression of D43 stabilized the active PSII units to a large extent under the salt-stress conditions. These results were in accordance with previous findings in heat-stressed wheat plants (Mathur et al. 2011) subjected to high salt stress (Mehta et al. 2010), *Arabidopsis* plants exposed to osmotic stress (Gururani et al. 2017), and melatonin-treated oats plants under osmotic stress conditions (Onoud Alyammahi and Gururani 2020).

Overall, based on the findings of this study, the possible mechanism of action in D43 plants under salinity stress can be summarized in a hypothetical model (Figure 6). The overexpression of the cytosolic *GAPDH* gene from potato in *Arabidopsis* plants, under salt stress, can lead to a signal transduction that in turn induces gene expression of several major stress-responsive components. These include the ROS-scavenging enzymes, proline biosynthetic pathway gene *P5CS1,* and several well-known abiotic stress-

responsive genes. Additionally, the overexpression of *D43* appears to induce photo-protective effects that lead to improved PSII efficiency and increased pigment accumulation under salinity stress. Collectively, these improved characteristic in D43 plants facilitated the amelioration of salinity stress.

5. Conclusion

GAPDH plays a crucial role as a key enzyme in glycolysis and gluconeogenesis, and has also been demonstrated to play a significant role in the growth of the primary root, aerial part of the plant, and in the production of ATP required for starch metabolism, along with phosphoglycerol kinase, as well as, fertility in *Arabidopsis*. Abiotic stress conditions induce the expression of GAPDH, which may be a natural mechanism by which crop plants adapt to the altered conditions. It may pave the way for acquiring additional energy for cellular adjustment required for plant growth in stress conditions, which is confirmed by transcriptome and metabolomics analysis, which shows that absence of GAPDH in plants can negatively affect synthesis of major plant metabolites. Taken together, based on previous reports and our findings, we propose that enhanced expression of *StD43*in higher plants plays a key role in the maintenance of PSII machinery and the ROS scavenging mechanism during salinity stress. Hence, we propose that this gene be used to develop stress-resistant crop plants; but further studies, particularly on experimental fields, are needed prior to extending its application to other crops.

Acknowledgment

Concept and design of experiments: MAG, SK, JV. Performance of experiments: OA, SK, AA, MAG. Analyzing of data: MAG JV SK, SS. Author of manuscript: MAG, SS.

Disclosure statement

No potential conflict of interest was reported by the author(s).

Funding

This work was supported by UAE University, KCGEB Center based [grant numbers 31R219 and 31R240].

Notes on contributors

Dr. Sajeesh Kappachery holds a PhD from Konkuk University, South Korea and is currently working as a Postdoctoral Fellow in the Biology department, UAE University.

Dr. Shina Sasi obtained her PhD from the Indian Institute of Spices Research, Kerala, India. She is currently working as a Research Associate at the Khalifa Center for Genetic Engineering and Biotechnology, affiliated to the UAE University.

Ms. Onoud Alyammahi has recently graduated as a MS student from the Biology department, UAE University. Her MS thesis was supervised by Dr. Mayank Gururani.

Ms. Ayesha Alyassi graduated with an undergraduate degree in Biology from UAE University. She did her research project under the supervision of Dr. Mayank Gururani.

Dr. Jelli Venkatesh is a Senior Researcher at Seoul National University, Korea. He obtained his PhD from Konkuk University, Korea and has expertise in Plant Biotechnology, Genomics and Molecular Breeding.

Dr. Mayank Anand Gururani is a plant biologist who is interested in understanding the molecular mechanism of photosynthetic components in higher plants exposed to abiotic stresses. He obtained his PhD in Molecular Biotechnology from Konkuk University, Seoul, Korea. He pursued his postdoctoral research at Jeju National University, Jeju Korea, followed by a one-year stint as Research Professor at Yeungnam University, Korea. He joined the UAE University in 2016 as Assistant Professor and currently he is serving as Associate Professor in the Biology department, UAE University.

ORCID

Mayank Anand Gururani http://orcid.org/0000-0003-4254-6450

References

Abdelaal KA, EL-Maghraby LM, Elansary H, Hafez YM, Ibrahim EI, El-Banna M, El-Esawi M, Elkelish A. 2020. Treatment of sweet pepper with stress tolerance-inducing compounds alleviates salinity stress oxidative damage by mediating the physio-biochemical activities and antioxidant systems. Agronomy. 10(1):26.

Ahanger MA, Aziz U, Alsahli AA, Alyemeni MN, Ahmad P. 2020. Influence of exogenous salicylic acid and nitric oxide on growth, photosynthesis, and ascorbate-glutathione cycle in salt stressed vigna angularis. Biomolecules. 10(1):42.

Ahmad P, Jaleel CA, Salem MA, Nabi G, Sharma S. 2010. Roles of enzymatic and nonenzymatic antioxidants in plants during abiotic stress. Crit Rev Biotechnol. 30(3):161–175.

Akilan S, Halima TH, Sasi S, Kappachery S, Baniekal-Hiremath G, Venkatesh J, Gururani MA. 2019. Evaluation of osmotic stress tolerance in transgenic Arabidopsis plants expressing Solanum tuberosum D200 gene. J Plant Interact. 14(1):79–86.

Alam P, Albalawi TH, Altalayan FH, Bakht MA, Ahanger MA, Raja V, Ashraf M, Ahmad P. 2019. 24-epibrassinolide (EBR) confers tolerance against NaCl stress in soybean plants by up-regulating antioxidant system, ascorbate-glutathione cycle, and glyoxalase system. Biomolecules. 9(11):640.

Alavilli H, Awasthi JP, Rout GR, Sahoo L, Lee BH, Panda SK. 2016. Overexpression of a Barley aquaporin gene, HvPIP2;5 confers salt and osmotic stress tolerance in yeast and plants. Front Plant Sci. 7 (OCTOBER2016):1–12.

Alyammahi O, Gururani MA. 2020. Chlorophyll-a fluorescence analysis reveals differential response of photosynthetic machinery in melatonin-treated oat plants exposed to osmotic stress. Agronomy. 10 (10):1520.

Azarabadi S, Abdollahi H, Torabi M, Salehi Z, Nasiri J. 2017. ROS generation, oxidative burst and dynamic expression profiles of ROS-scavenging enzymes of superoxide dismutase (SOD), catalase (CAT) and ascorbate peroxidase (APX) in response to Erwinia amylovora in pear (Pyrus communis L). Eur J Plant Pathol [Internet. 147 (2):279–294. doi:10.1007/s10658-016-1000-0.

Blankenagel S, Yang Z, Avramova V, Schön CC, Grill E. 2018. Generating plants with improved water use efficiency. Agronomy. 8(9):194.

Brini F, Hanin M, Mezghani I, Berkowitz GA, Masmoudi K. 2007. Overexpression of wheat Na+/H+ antiporter TNHX1 and H+-pyrophosphatase TVP1 improve salt- and drought-stress tolerance in Arabidopsis thaliana plants. J Exp Bot. 58(2):301–308.

Calvin M. 1962. The path of carbon in photosynthesis. Science. 135:879–889.

Cantero A, Barthakur S, Bushart TJ, Chou S, Morgan RO, Fernandez MP, Clark GB, Roux SJ. 2006. Expression profiling of the Arabidopsis annexin gene family during germination, de-etiolation and abiotic stress. Plant Physiol Biochem. 44(1):13–24.

Cerff R, Chambers S. 1979. Subunit structure dehydrogenases of higher. J Biol Chem. 254(13):6094–6098.

Chen Y, Li C, Zhang B, Yi J, Yang Y, Kong C, Lei C, Gong M. 2019. The role of the late embryogenesis-abundant (LEA) protein family in development and the abiotic stress response: a comprehensive expression analysis of potato (Solanum tuberosum). Genes (Basel. 10(2):1–16.

Choi B, Ghosh R, Gururani MA, Shanmugam G, Jeon J, Kim J, Park S-C, Jeong M-J, Han K-H, Bae D-W, Bae H. 2017. Positive regulatory

role of sound vibration treatment in Arabidopsis thaliana against Botrytis cinerea infection. Sci Rep. 7(1):1–14.
Choudhary NL, Sairam RK, Tyagi A. 2005. Expression of Δ ^{1}-pyrroline-5-carboxylate synthetase gene during drought in rice (Oryza sativa L.). Indian J Biochem Bio. 42(6):366–370.
Corpet F. 1988. Multiple sequence alignment with hierarchical clustering. Nucleic Acids Res. 16(22):10881–10890.
Finkelstein RR. 2010. The role of hormones during seed development and germination. In: Plant hormones. Dordrecht: Springer; p. 549–573.
Fricke W, Peters WS. 2002. The biophysics of leaf growth in salt-stressed barley. A study at the cell level. Plant Physiol. 129(1):374–388.
Fu J, Huang B. 2001. Involvement of antioxidants and lipid peroxidation in the adaptation of two cool-season grasses to localized drought stress. Environ Exp Bot. 45:105–114.
Fu Y, Kawasaki T, Shimamoto K, Yang Z. 2018. ROP/RACGTPases. [place unknown].
Ghosh R, Gururani MA, Ponpandian LN, Mishra RC, Park SC, Jeong MJ, Bae H. 2017. Expression analysis of sound vibration-regulated genes by touch treatment in arabidopsis. Front Plant Sci. 8:100.
Goltsev V, Zaharieva I, Chernev P, Kouzmanova M, Kalaji HM, Yordanov I, Krasteva V, Alexandrov V, Stefanov D, Allakhverdiev SI, Strasser RJ. 2012. Drought-induced modifications of photosynthetic electron transport in intact leaves: analysis and use of neural networks as a tool for a rapid non-invasive estimation. Biochim Biophys Acta - Bioenerg. 1817(8):1490–1498.
Guo L, Yang H, Zhang X, Yang S. 2013. Lipid transfer protein 3 as a target of MYB96 mediates freezing and drought stress in Arabidopsis. J Exp Bot. 64(6):1755–1767.
Gupta R. 2020. The oxygen-evolving complex: a super catalyst for life on earth, in response to abiotic stresses. Plant Signal Behav [Internet]. 15(12). doi:10.1080/15592324.2020.1824721
Gururani MA, Upadhyaya CP, Strasser RJ, Yu JW, Park SW. 2013a. Evaluation of abiotic stress tolerance in transgenic potato plants with reduced expression of PSII manganese stabilizing protein. Plant Sci. 198:7–16.
Gururani MA, Upadhyaya CP, Baskar V, Venkatesh J, Nookaraju A, Park SW. 2013b. Plant growth-promoting rhizobacteria enhance abiotic stress tolerance in Solanum tuberosum through inducing changes in the expression of ROS-scavenging enzymes and improved photosynthetic performance. J Plant Growth Regul. 32(2):245–258.
Gururani MA, Venkatesh J, Ganesan M, Strasser RJ, Han Y, Il KJ, Lee HY, Song PS. 2015a. In vivo assessment of cold tolerance through chlorophyll-a fluorescence in transgenic zoysiagrass expressing mutant phytochrome A. PLoS One. 10(5):1–17.
Gururani MA, Venkatesh J, Ghosh R, Strasser RJ, Ponpandian LN, Bae H. 2017. Chlorophyll-a fluorescence evaluation of PEG-induced osmotic stress on PSII activity in *Arabidopsis* plants expressing *SIP1*. Plant Biosyst - An Int J Deal with all Asp Plant Biol [Internet]. 3504(December):1–8. https://www.tandfonline.com/doi/full/10.1080/11263504.2017.1403392.
Gururani MA, Venkatesh J, Tran LSP. 2015b. Regulation of photosynthesis during abiotic stress-induced photoinhibition. Mol Plant [Internet]. 8(9):1304–1320. doi:10.1016/j.molp.2015.05.005.
Harper JT, Keeling PJ. 2003. Nucleus-encoded, plastid-targeted glyceraldehyde-3-phosphate dehydrogenase (GAPDH) indicates a single origin for chromalveolate plastids. Mol Biol Evol. 20(10):1730–1735.
Heldt H, Piechulla B. 2011. Photosynthetic CO2 assimilation by the Calvin cycle. In: Heldt HW, Piechulla B, editors. Plant biochem. London: Academic Press; p. 163–191.
Hmida-Sayari A, Gargouri-Bouzid R, Bidani A, Jaoua L, Savoure A, Jaoua S. 2005. Overexpression of D 1 -pyrroline-5-carboxylate synthetase increases proline production and confers salt tolerance in transgenic potato plants. Plant Sci. 169:746–752.
Huang W, Zhang S, Wu G, Yu Y, Ren C, Kang Q, Liu Y, Liang C, Zhang L, Zhan Y. 2019. Transcriptome profiling of potassium starvation responsiveness in flax (Linum usitatissimum L. Pakistan J Bot. 51 (3):865–878.
Hussain S, Khaliq A, Tanveer M, Matloob A, Hussain HA. 2018. Aspirin priming circumvents the salinity-induced effects on wheat emergence and seedling growth by regulating starch metabolism and antioxidant enzyme activities. Acta Physiol Plant. 40(4):1–12.
Jain M, Nijhawan A, Tyagi AK, Khurana JP. 2006. Validation of housekeeping genes as internal control for studying gene expression in rice by quantitative real-time PCR. Biochem Biophys Res Commun. 345 (2):646–651.
Kalaji HM, Carpentier R, Allakhverdiev SI, Bosa K. 2012. Fluorescence parameters as early indicators of light stress in barley. J Photochem Photobiol B Biol [Internet]. 112:1–6. doi:10.1016/j.jphotobiol.2012.03.009.
Kalaji HM, Govindjee, Bosa K, Kościelniak J, Zuk-Gołaszewska K. 2011. Effects of salt stress on photosystem II efficiency and CO2 assimilation of two Syrian barley landraces. Environ Exp Bot. 73(1):64–72.
Kalaji HM, Jajoo A, Oukarroum A, Brestic M, Zivcak M, Samborska IA, Cetner MD, Łukasik I, Goltsev V, Ladle RJ. 2016. Chlorophyll a fluorescence as a tool to monitor physiological status of plants under abiotic stress conditions. Acta Physiol Plant. 38(4):102.
Kalaji HM, Oukarroum A, Alexandrov V, Kouzmanova M, Brestic M, Zivcak M, Samborska IA, Cetner MD, Allakhverdiev SI, Goltsev V. 2014. Identification of nutrient deficiency in maize and tomato plants by invivo chlorophyll a fluorescence measurements. Plant Physiol Biochem. 81:16–25.
Kappachery S, Baniekal-Hiremath G, Yu JW, Park SW. 2015. Effect of over-and under-expression of glyceraldehyde 3-phosphate dehydrogenase on tolerance of plants to water-deficit stress. Plant Cell Tissue Organ Cult. 121(1):97–107.
Kappachery S, Yu JW, Baniekal-Hiremath G, Park SW. 2013. Rapid identification of potential drought tolerance genes from Solanum tuberosum by using a yeast functional screening method. Comptes Rendus - Biol [Internet. 336(11–12):530–545. doi:10.1016/j.crvi.2013.09.006.
Kawasaki T, Henmi K, Ono E, Hatakeyama S, Iwano M, Satoh H, Shimamoto K. 1999. The small GTP-binding protein Rac is a regulator of cell death in plants. Proc Natl Acad Sci U S A. 96 (19):10922–10926.
Kaya C, Higgs D, Ashraf M, Alyemeni MN, Ahmad P. 2020. Integrative roles of nitric oxide and hydrogen sulfide in melatonin-induced tolerance of pepper (Capsicum annuum L.) plants to iron deficiency and salt stress alone or in combination. Physiol Plant. 168(2):256–277.
Khaliq A, Zia-ul-Haq M, Ali F, Aslam F, Matloob A, Navab A, Hussain S. 2015. Salinity tolerance in wheat cultivars Is related to enhanced activities of enzymatic antioxidants and reduced lipid peroxidation. clean - soil, Air. Water (Basel). 43(8):1248–1258.
Khan I, Raza MA, Awan SA, Shah GA, Rizwan M, Ali B, Tariq R, Hassan MJ, Alyemeni MN, Brestic M, et al. 2020. Amelioration of salt induced toxicity in pearl millet by seed priming with silver nanoparticles (AgNPs): the oxidative damage, antioxidant enzymes and ions uptake are major determinants of salt tolerant capacity. Plant Physiol Biochem. 156(July):221–232.
Kohli SK, Khanna K, Bhardwaj R, Abd Allah EF, Ahmad P, Corpas FJ. 2019. Assessment of subcellular ROS and NO metabolism in higher plants: multifunctional signaling molecules. Antioxidants. 8(12):641.
Kong L, Huo H, Mao P. 2015. Antioxidant response and related gene expression in aged oat seed. Front Plant Sci. 6(March):1–9.
Konopka-Postupolska D, Clark G, Goch G, Debski J, Floras K, Cantero A, Fijolek B, Roux S, Hennig J. 2009. The role of annexin 1 in drought stress in Arabidopsis. Plant Physiol. 150(3):1394–1410.
Kumar D, Singh H, Raj S, Soni V. 2020. Chlorophyll a fluorescence kinetics of mung bean (Vigna radiata L.) grown under artificial continuous light. Biochem Biophys Reports [Internet]. 24. doi:10.1016/j.bbrep.2020.100813
Kumar M, Choi J, An G, Kim S-R. 2017. Ectopic expression of OsSta2 enhances salt stress tolerance in rice. Front Plant Sci [Internet]. 8 (March):1–14. http://journal.frontiersin.org/article/10.3389/fpls.2017.00316/full.
De Las Rivas J, Heredia P, Roman A. 2007. Oxygen-evolving extrinsic proteins (PsbO,P,Q,R): bioinformatic and functional analysis. Biochim Biophys Acta - Bioenerg. 1767(6):575–582.
Lindemose S, O'Shea C, Jensen MK, Skriver K. 2013. Structure, function and networks of transcription factors involved in abiotic stress responses. Int J Mol Sci. 14(3):5842–5878.
Liu Y, Pan T, Tang Y, Zhuang Y, Liu Z, Li P, Li H, Huang W, Tu S, Ren G, et al. 2020. Proteomic analysis of rice subjected to low light stress and overexpression of OsGAPB increases the stress tolerance. Rice. 13:1–10.
Maeda HA, Fernie AR. 2021. Evolutionary history of plant metabolism. Annu Rev Plant Biol. 72:185–216.

Mathur S, Jajoo A, Mehta P, Bharti S. 2011. Analysis of elevated temperature-induced inhibition of photosystem II using chlorophyll a fluorescence induction kinetics in wheat leaves (Triticum aestivum). Plant Biol (Stuttg) [Internet]. 13(1):1–6. [accessed 2014 Feb 10] http://www.ncbi.nlm.nih.gov/pubmed/21143718.

Mehta P, Jajoo A, Mathur S, Bharti S. 2010. Chlorophyll a fl uorescence study revealing effects of high salt stress on photosystem II in wheat leaves. Plant Physiol Biochem [Internet]. 48(1):16–20. doi:10.1016/j.plaphy.2009.10.006.

Muñoz-Bertomeu J, Cascales-Miñana B, Alaiz M, Segura J, Ros R. 2010. A critical role of plastidial glycolytic glyceraldehyde-3-phosphate dehydrogenase in the control of plant metabolism and development. Plant Signal Behav. 5(1):67–69.

Nath K, Jajoo A, Poudyal RS, Timilsina R, Park YS, Aro E-M, Nam HG, Lee C-H. 2013. Towards a critical understanding of the photosystem II repair mechanism and its regulation during stress conditions. FEBS Lett [Internet]. 587(21):3372–3381. [accessed 2014 Mar 5] http://www.ncbi.nlm.nih.gov/pubmed/24056074.

Noctor G, Mhamdi A, Foyer CH. 2014. The roles of reactive oxygen metabolism in drought: not so cut and dried. Plant Physiol [Internet]. 164(4):1636–1648. http://www.plantphysiol.org/cgi/doi/10.1104/pp.113.233478.

Oukarroum A, El Madidi S, Strasser RJ. 2012. Exogenous glycine betaine and proline play a protective role in heat-stressed barley leaves (Hordeum vulgare L.): A chlorophyll a fluorescence study. Plant Biosyst. 146(4):1037–1043.

Pan Y, Li J, Jiao L, Li C, Zhu D, Yu J. 2016. A non-specific Setaria italica lipid transfer protein gene plays a critical role under abiotic stress. Front Plant Sci. 7(NOVEMBER2016):1–15.

Papageorgiou GC, Govindjee. 2014. Non-photochemical quenching and energy dissipation in plants, Algae and Cyanobacteria. In: Demmig-Adams B, editor. Non-photochemical quenching and energy dissipation in plants, Algae and Cyanobacteria [Internet]. [place unknown]: Springer, Dordrecht; p. 1–44. http://link.springer.com/10.1007/978-94-017-9032-1

Per TS, Khan NA, Reddy PS, Masood A, Hasanuzzaman M, Khan MIR, Anjum NA. 2017. Approaches in modulating proline metabolism in plants for salt and drought stress tolerance: phytohormones, mineral nutrients and transgenics. Plant Physiol Biochem. 115:126–140.

Puyang X, An M, Han L, Zhang X. 2015. Protective effect of spermidine on salt stress induced oxidative damage in two Kentucky bluegrass (Poa pratensis L.) cultivars. Ecotoxicol Environ Saf [Internet]. 117:96–106. doi:10.1016/j.ecoenv.2015.03.023.

Qin T, Tian Q, Wang G, Xiong L. 2019. Lower temperature 1 enhances ABA responses and plant drought tolerance by modulating the stability and localization of C2-domain ABA-related proteins in arabidopsis. Mol Plant [Internet]. 12(9):1243–1258. doi:10.1016/j.molp.2019.05.002.

Rius SP, Casati P, Iglesias AA, Gomez-Casati DF. 2006. Characterization of an Arabidopsis thaliana mutant lacking a cytosolic non-phosphorylating glyceraldehyde-3-phosphate dehydrogenase. Plant Mol Biol. 61(6):945–957.

Rodriguez L, Gonzalez-Guzman M, Diaz M, Rodrigues A, Izquierdo-Garcia AC, Peirats-Llobet M, Fernandez MA, Antoni R, Fernandez D, Marquez JA, et al. 2014. C2-domain abscisic acid-related proteins mediate the interaction of PYR/PYL/RCAR abscisic acid receptors with the plasma membrane and regulate abscisic acid sensitivity in arabidopsis. Plant Cell. 26(12):4802–4820.

Salim Akhter M, Noreen S, Mahmood S, Athar H ur R, Ashraf M, Abdullah Alsahli A, Ahmad P. 2021. Influence of salinity stress on PSII in barley (Hordeum vulgare L.) genotypes, probed by chlorophyll-a fluorescence. J King Saud Univ - Sci [Internet] 33(1). doi:10.1016/j.jksus.2020.101239

Sasi S, Venkatesh J, Daneshi R, Gururani M. 2018. Photosystem II extrinsic proteins and their putative role in abiotic stress tolerance in higher plants. Plants [Internet]. 7(4):100. http://www.mdpi.com/2223-7747/7/4/100.

Sirhindi G, Mir MA, Abd-Allah EF, Ahmad P, Gucel S. 2016. Jasmonic acid modulates the physio-biochemical attributes, antioxidant enzyme activity, and gene expression in glycine max under nickel toxicity. Front Plant Sci. 7(MAY2016):1–12.

Skubacz A, Daszkowska-Golec A, Szarejko I. 2016. The role and regulation of ABI5 (ABA-insensitive 5) in plant development, abiotic stress responses and phytohormone crosstalk. Front Plant Sci. 7 (DECEMBER2016):1–17.

Sreenivasulu N, Grimm B, Wobus U, Weschke W. 2000. Differential response of antioxidant compounds to salinity stress in salt-tolerant and salt-sensitive seedlings of foxtail millet (Setaria italica). Physiol Plant. 109(4):435–442.

Strasser RJ, Srivastava A, Govindjee. 1995. Polyphasic chlorophyll a fluorescence transient in plant and cyanobacteria*. Photochem Photobiol. 61(1):32–42.

Suzuki Y, Ishiyama K, Sugawara M, Suzuki Y, Kondo E, Takegahara-Tamakawa Y, Yoon DK, Suganami M, Wada S, Miyake C, Makino A. 2021. Overproduction of chloroplast glyceraldehyde-3-phosphate dehydrogenase improves photosynthesis slightly under elevated [CO2] conditions in rice. Plant Cell Physiol. 62(1):156–165.

Takahashi S, Badger MR. 2011. Photoprotection in plants: a new light on photosystem II damage. Trends Plant Sci [Internet]. 16(1):53–60. [accessed 2014 Mar 4] http://www.cell.com/trends/plant-science/fulltext/S1360-1385(10)00211-6.

Varghese N, Alyammahi O, Nasreddine S, Alhassani A, Gururani MA. 2019. Melatonin positively influences the photosynthetic machinery and antioxidant system of avena sativa during salinity stress. Plants. 8(12):610.

Vuletic V, Spanic V. 2019. Characterization of photosynthetic performance during natural leaf senescence in winter wheat : multivariate analysis as a tool for phenotypic characterization characterization of photosynthetic performance during natural leaf senescence in winter wheat. Photosynthetica. 57:116–128.

Xiao W, Wang H, Liu W, Wang X, Guo Y, Strasser RJ, Qiang S, Chen S, Hu Z. 2020. Action of alamethicin in photosystem II probed by the fast chlorophyll fluorescence rise kinetics and the JIP-test. Photosynthetica. 58(Special Issue):358–368.

Yokotani N, Ichikawa T, Kondou Y, Maeda S, Iwabuchi M, Mori M, Hirochika H, Matsui M, Oda K. 2009. Overexpression of a rice gene encoding a small C2 domain protein OsSMCP1 increases tolerance to abiotic and biotic stresses in transgenic arabidopsis. Plant Mol Biol. 71(4–5):391–402.

Yoshida T, Mogami J, Yamaguchi-Shinozaki K. 2014. ABA-dependent and ABA-independent signaling in response to osmotic stress in plants. Curr Opin Plant Biol [Internet]. 21:133–139. doi:10.1016/j.pbi.2014.07.009.

Yusuf MA, Kumar D, Rajwanshi R, Strasser RJ, Tsimilli-Michael M, Govindjee, Sarin NB. 2010. Overexpression of gamma-tocopherol methyl transferase gene in transgenic Brassica juncea plants alleviates abiotic stress: physiological and chlorophyll a fluorescence measurements. Biochim Biophys Acta [Internet] 1797(8):1428–1438. [accessed 2014 Feb 5] http://www.ncbi.nlm.nih.gov/pubmed/20144585

Zhang X, Henriques R, Lin SS, Niu QW, Chua NH. 2006. Agrobacterium-mediated transformation of Arabidopsis thaliana using the floral dip method. Nat Protoc. 1(2):641–646.

Zhang XH, Rao XL, Shi HT, Li RJ, Lu YT. 2011. Overexpression of a cytosolic glyceraldehyde-3-phosphate dehydrogenase gene OsGAPC3 confers salt tolerance in rice. Plant Cell Tissue Organ Cult. 107(1):1–11.

Zhang Y, Li Z, Peng Y, Wang X, Peng D, Li Y, He X, Zhang X, Ma X, Huang L, Yan Y. 2015. Clones of FeSOD, MDHAR, DHAR genes from white clover and gene expression analysis of ROS-scavenging enzymes during abiotic stress and hormone treatments. Molecules. 20(11):20939–020954.

Zivcak M, Brestic M, Kalaji HM, Govindjee. 2014a. Photosynthetic responses of sun- and shade-grown barley leaves to high light: Is the lower PSII connectivity in shade leaves associated with protection against excess of light? Photosynth Res. 119(2014):339–354.

Zivcak M, Kalaji HM, Shao HB, Olsovska K, Brestic M. 2014b. Photosynthetic proton and electron transport in wheat leaves under prolonged moderate drought stress. J Photochem Photobiol B Biol. 137:107–115.

Zou HW, Tian XH, Ma GH, Li ZX. 2013. Isolation and functional analysis of ZmLTP3, a homologue to Arabidopsis LTP3. Int J Mol Sci. 14(3):5025–5035.